A Doppler broadening positron annihilation spectroscopy study of magnetically induced recovery in nickel

1993 J. Phys.: Condens. Matter 5 4563

(http://iopscience.iop.org/0953-8984/5/26/026)

J. Phys.: Condens. Matter 5 (1993) 4563–4572. Printed in the UK

A Doppler broadening positron annihilation spectroscopy study of magnetically induced recovery in nickel

Rajan Vaidyanathan†, James P Schaffer† and Buncha Thanaboonsombut‡

† Chemical Engineering, Lafayette College, Easton, PA 18042, USA

‡ Materials Engineering, Georgia Institute of Technology, Atlanta, GA 30332, USA

Received 24 July 1992, in final form 10 March 1993

Abstract. Doppler broadening positron annihilation spectroscopy and x-ray diffraction have been used to investigate the effects of pulsed magnetic fields on the defect structure of heavily cold worked nickel samples. The experimental variables under investigation include temperature, crystallographic texture, magnetic field strength and frequency. The key results can be summarized as follows: (i) the extent of the magnetically induced recovery, although small compared with that of thermal recovery, is significant; (ii) the pulsed magnetic field appears to have a greater effect on dislocation density than on point-defect concentration; and (iii) texture and temperature are important experimental variables (the effects of pulsing frequency and field strength could not be separated due to experimental limitations).

1. Introduction

Previous investigations have shown that the application of an external magnetic field can influence both the mechanical and physical properties of metals [1–5]. The magnitude of the magnetically induced changes in properties can be significant in ferromagnetic metals and their alloys. It has also been demonstrated by Su *et al* [6] that positron annihilation spectroscopy can be used to study the changes in the atomic scale defect structure induced by pulsed magnetic fields. The specific goals of this work were: (i) to identify the relevant changes in the defect structure of heavily cold worked nickel when subjected to a pulsed magnetic field; and (ii) to determine the important processing variables that influence the extent of the magnetically induced defect recovery process.

2. Background

2.1. Positron annihilation spectroscopy (PAS)

PAS is a non-contact and non-destructive technique that can be used to characterize the atomic scale defect structure of materials [7–8]. When a positron is injected into a sample it quickly reaches thermal velocities and diffuses through the lattice until it eventually annihilates with an electron to produce (usually) two γ-rays. If both particles were at rest, conservation of momentum and energy would require the two γ-rays to be emitted in exactly opposite directions, each with an energy of 511 keV corresponding to the rest mass of an electron (or positron). When the annihilation event occurs, however, the non-zero net momentum of the electron/positron pair modifies the characteristics of the annihilation radiation. The two

0953-8984/93/264563+10$07.50

γ-rays will no longer be emitted anti-parallel to one another and their characteristic energy will be altered from 511 keV. The technique which measures the energy deviations from 511 keV is known as Doppler broadening PAS (DBPAS).

Due to the relative velocities of the positron and electron just prior to annihilation, the energy deviations from 511 keV are dominated by the momenta of the electrons. Since the electron momentum distribution at a defect site is characteristic of that defect, the Doppler PAS energy lineshape is in fact a 'fingerprint' of the defect structure in the material. Thus, under some circumstances by monitoring changes in the Doppler PAS lineshape it is possible to track changes in defect types and/or defect concentrations.

2.2. *Sample selection*

The sample selected was polycrystalline nickel of 99.998% purity, supplied by Material Research Corporation. Nickel shows a stable dislocation structure during long-term storage at room temperature, as confirmed by Mackenzie [9]. The Curie temperature of ferromagnetic nickel is 631 K, the saturation magnetization at room temperature being 4.84×10^5 A m^{-1}. Nickel also has relatively large magnetostriction constants among ferromagnetic materials and hence the interaction between dislocations and domain walls is expected to be significant. The magnetocrystalline anisotropy of nickel results in $\langle 111 \rangle$ being an easy direction of magnetization, $\langle 110 \rangle$ intermediate and $\langle 100 \rangle$ hard; the magnetocrystalline anisotropy constants K_1, K_2 being -4.5×10^3 J m^{-3} and 2.4×10^3 J m^{-3}, respectively, at room temperature. Domain walls can be characterized by the angle between the magnetization vectors in the domains on either side of the wall. The important types of domain walls in nickel are 70.53° walls lying in {100} and {110} planes, 109.47° walls lying in {100}, {110} and {111} planes and 180° walls lying in {110} and {112} planes. The above values have been obtained from [10, 11].

3. Experimental procedures

3.1. *PAS*

The system used to acquire the Doppler PAS data has been described previously by Su *et al* [6]. The energy dispersion was 64 eV per channel and each spectrum contained 201 channels for a total width of 511 ± 6.4 keV. The data collection was terminated when 20 000 counts were recorded in the peak channel. This corresponded to approximately 1.2 million counts in each spectrum and required about 40 min per experiment.

Each energy spectrum was characterized by the standard S- and R-parameters [12, 13]. The S-parameter is defined as the ratio of the number of counts in a fixed central energy window to the total number of counts in the spectrum. The central energy window was 31 channels wide and extended over the region 511 ± 0.96 keV. The R-parameter utilizes the sum of the number of counts in two symmetrically located wing regions of the energy spectrum and the number of counts in a central energy window. The wing regions were each 32 channels wide (2.048 keV) and began 28 channels (1.792 keV) on either side of the spectrum centroid. The central window was 17 channels wide and extended over the region 511 ± 0.512 keV. If N_w and N_c represent the sum of the number of counts in the two-wing regions and the number of counts in the central energy window, respectively, each divided by the total number of counts in the spectrum, then the R-parameter is defined as

$$R = |(N_c^s - N_c^r)/(N_w^s - N_w^r|$$

where the superscripts s and r refer to the sample under investigation and a 'defect-free' reference sample, respectively. The reference samples used in this work are a pair of nickel specimens that have been annealed at 500 °C for 1 h and then slowly cooled to room temperature. This sample was chosen as the reference since it gave the lowest value of the PAS S-parameter (see figure 3 later).

A constant value of R, when accompanied by a changing value of S, signifies the presence of a single dominant defect trap, while a change in R suggests a change in the dominant defect type. For a single dominant defect trap an increase in S usually implies an increase in the defect concentration. The S- and R-parameters reported in this work represent the average values of at least three PAS experiments for each pair of samples. The error bars shown in the figures represent plus-and-minus one standard deviation for these average values.

Before being able to use the S- and R-parameters to describe magnetically induced changes in defect structures it is important to obtain reference values for the PAS parameters using carefully prepared samples. As described in more detail below, the necessary reference values were obtained using both quenched and cold worked nickel samples.

3.2. X-ray diffraction (XRD)

The experiments were performed using a Philips PW1800 automated diffraction system. A copper radiation source was used with an operating voltage of 40 kV and a current of 30 mA. A step size of 0.01° and a sampling time of 1 s were used to scan the range from 40° to 90°. Pole figure experiments were done to confirm the texture present in a given sample. The (111), (200), and (220) reflections corresponding to 44.6°, 52.0° and 76.5°, were observed.

3.3. Sample preparation

The material investigated was cut from a cylindrical rod approximately 1.2 cm in diameter. Since it was found that crystallographic texture is an important variable, the methods used to develop the desired textures will be described. We note that the PAS results depend very strongly on the sample preparation procedure.

Process A. $\{132\}\langle 112\rangle$ texture development.

Step 1. Cut a disc of thickness 1.2 cm from rod.

Step 2. Sequentially cold roll disc in a direction perpendicular to the original axis of the rod to a final thickness $\sim$ 6 mm in steps $\sim$ 1 mm per pass.

Step 3. Heat treat at 950 °C for 1 h in argon.

Step 4. Water quench to room temperature.

Step 5. Electropolish using 80% concentration H_2SO_4 with an applied voltage of 12 V and an operating current $\sim$ 2 A.

Step 6. Sequentially cold roll the disc in a direction perpendicular to the original axis of the rod to a final reduction of area of 80%. For the deformation procedure used in this work the reduction in cross sectional area is equivalent to the thickness reduction. That is, the per cent reduction in area (%RA) is given by $\%RA = [(t_0 - t_f)/t_0] \times 100$ where T_0 and t_f are the original and final thicknesses of the cold worked sample.

Process B. $\{100\}\langle 001\rangle + \{121\}\langle 011\rangle$ texture development.

Step 1. Cut a disc of thickness 1.2 cm from rod.

Step 2. Sequentially cold roll disc in a direction parallel to the original axis of the rod to a final thickness $\sim$ 6 mm in steps $\sim$ 1 mm per pass.

Step 3. Heat treat at 700 °C for 1 h in argon.
Step 4. Furnace cool (about 5 h) to room temperature.
Step 5. Electropolish using the same conditions as in process A.
Step 6. Cold roll to a final reduction of area of 80%, as in process A.

The samples for PAS measurements were then cut to dimensions ~ 1 cm$\times \sim 1$ cm and had a final thickness ~ 1.2 mm.

3.4. Pulsed magnetic field treatment

The pulsed magnetic fields were generated by a fluxatron model U-102 obtained from Innovex Corporation. This device consists of a magnetic coil that can provide several different field strengths. The samples were loaded in the fluxatron so that the axis of the coil coincided with the rolling direction. The magnetic treatments were performed either at room temperature or at 77 K.

The energy, emitted by the unit in a pulsed wave form, is absorbed by a specimen which is placed in a sliding tray in the centre of the coil. Each 'round' of energy output is fixed by a microprocessor within the fluxatron to a duration of 42 s. The two field strength settings investigated in this work were: (i) low field/high frequency, 80 Oe with 630 pulses per round (i.e. 630 pulses in 42 s); and (ii) high field/low frequency, 420 Oe with 79 pulses per round.

4. Results

Figures 1–3 show the results of the calibration experiments. Figure 1 is a plot of the PAS lineshape parameters S and R as a function of quench temperature. The starting materials for this series of experiments were samples that had been annealed at 400 °C for 1 h and furnace cooled for 5 h to room temperature. These samples were held at the various temperatures for 1 h and then water quenched to room temperature. Note that the figure also shows the equilibrium vacancy concentration at the elevated temperature, assuming a vacancy formation energy of 1.6 eV [14]. This information is included for a qualitative comparison only.

Figure 2 shows the change in S and R as a function of cold working, reported as per cent reduction in area (%RA). The starting materials were again fully annealed samples and the rolling procedure was similar to that described as process B in section 3.3.

The changes induced in S and R during an isochronal thermal annealing treatment are shown in figure 3. The starting material was cold worked to 80 %RA and the samples were held for 1 h at each of the temperatures indicated before being furnace cooled to room temperature. This figure also shows the change in hardness, reported using Rockwell scale A, for the same series of samples.

Figures 4–7 show how the PAS parameters are influenced by the interaction between a pulsed magnetic field and the atomic scale defect structure of nickel. In the first experiment fully annealed samples were held at 900 °C for 1 h and then water quenched to room temperature. These samples were then subjected to a series of magnetic treatments (low-field-strength/high-frequency) at room temperature. The S- and R-parameters for these samples are shown in figure 4.

In order to investigate the influence of texture on the extent of magnetic recovery two pairs of 80 %RA cold worked nickel samples, one with $\{132\}\langle 112\rangle$ texture and the other with $\{100\}\langle 001\rangle + \{121\}\langle 011\rangle$ texture, were subjected to a series of low-field/high-frequency

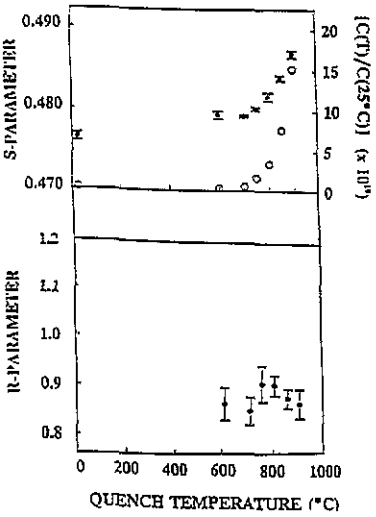

Figure 1. *S*- and *R*-parameters as a function of quench temperature. *Calculated vacancy concentrations*—$[C(T)/C(25\,^{\circ}C)]$—are included for comparison (open circles). The samples were held at the indicated temperature for 1 h and then water quenched to room temperature.

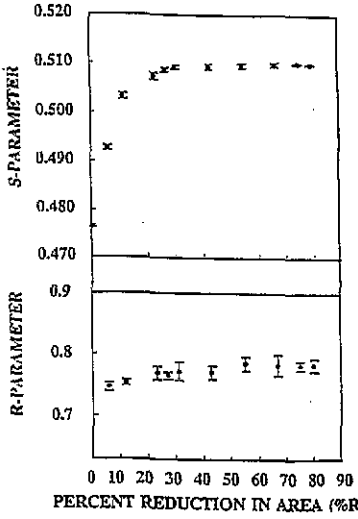

Figure 2. *S*- and *R*-parameters as a function of per cent *cold working (i.e. per cent reduction in area)*. Prior to cold working the samples were annealed and the rolling procedure was similar to that described as process B in section 3.3.

magnetic treatments at room temperature. The *S*- and *R*-parameters for these two pairs of samples are plotted as a function of the number of rounds of magnetic treatment in figure 5.

The effect of the temperature on the extent of magnetic recovery was studied by comparing the *S*- and *R*-parameters for two sets of samples treated at room temperature and 77 K, respectively. These results are shown in figure 6. The starting material was 80 %RA nickel with the {132}⟨112⟩ texture and the low-field/high-frequency magnetic treatment was employed. Although the magnetic processing was performed at two different temperatures all of the PAS measurements were done at room temperature.

Finally, the influence of magnetic field strength and frequency was investigated by comparing the results from the low-field/high-frequency and high-field/low-frequency settings described above. The *S*- and *R*-parameters for these two magnetic processing conditions are plotted as a function of the number of rounds of magnetic treatment in figure 7. The starting material was 80 %RA nickel with the {132}⟨112⟩ texture and the magnetic processing was performed at room temperature.

5. Discussion

The data in figure 1 indicate that the *S*-parameter is capable of tracking the point-defect concentration resulting from the quenching process. A constant *R*-parameter suggests that the dominant positron trap is the same for all of the quenching process. The increase in *S* is consistent with the increase in the calculated vacancy concentration and this suggests that

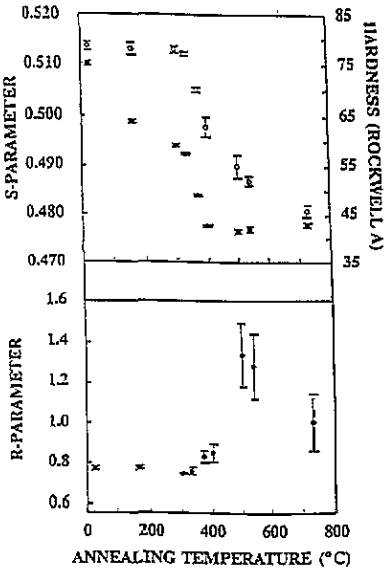

Figure 3. *S*- and *R*-parameters as a function of annealing temperature. Hardness values are included for comparison (open circles). The starting material was cold worked to 80 %RA and the samples were held for 1 h at each of the temperatures indicated before being furnace cooled to room temperature.

the dominant defects are vacancies and/or small vacancy clusters. The increase in *S* with %RA seen in figure 2 indicates an increase in the defect densities, possibly both dislocations and associated point-defect debris, resulting from the cold work process. The *R*-parameter is again constant but has a different value than that in the previous experiment, indicating a different dominant positron trap. Beyond 40 %RA the *S*-parameter is unable to respond to further increases in defect density. The saturation trapping effect occurs whenever the defect concentration is large enough that all positrons are trapped prior to annihilation from the bulk. The annealing curves in figure 3 display the classic recovery–recrystallization–grain-growth behaviour. The *R*-parameter shows two-step changes, corresponding to the change from the recovery stage ($\sim$ 150–300 °C) to the recrystallization stage ($\sim$ 300–400 °C) and from the recrystallization stage to the grain-growth stage ($\sim$ 400–720 °C) of the thermal anneal. The temperatures at which these changes occur are consistent with Clarebrough *et al* [15]. The data in figure 3 suggest that the *S*-parameter is more sensitive to the changes in the point-defect concentration during the recovery stage than the hardness measurements, while both measurements monitor the reduction in dislocation density during the recrystallization stage.

During grain growth, since the positron's random diffusion length is smaller than the grain size, the fraction of the positrons trapped at the grain boundaries is too small to significantly contribute to the *S*-parameter. Hence the *S*-parameter levels off above 400 °C. *R*-parameter analysis in this temperature range has limited physical significance since the value of *R* is approaching the indeterminate form 0/0 (refer to the equation defining *R* in section 3.1). The reason for this is that the atomic scale characteristics of the sample under investigation are nearly indistinguishable from those of the reference sample. Note

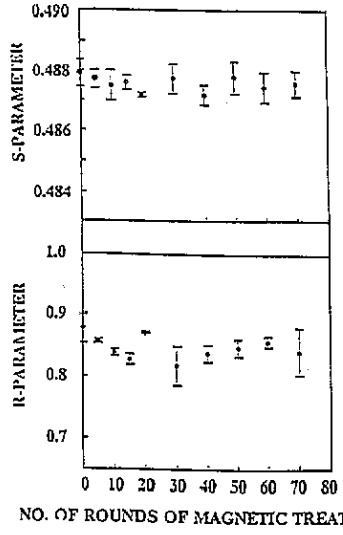

Figure 4. *S*- and *R*-parameters as a function of number of rounds of magnetic treatment (low-field/high-frequency) for the quenched nickel samples. The samples were fully annealed, reheated to 900 °C for 1 h, then water quenched to room temperature.

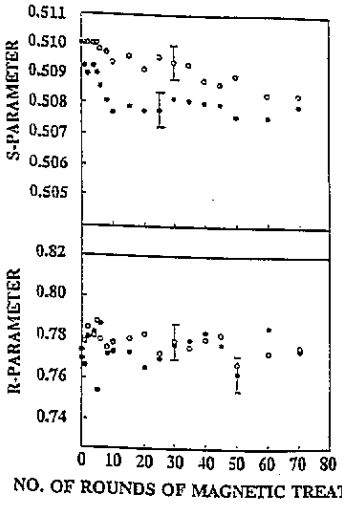

Figure 5. *S*- and *R*-parameters as a function of number of rounds of magnetic treatment for nickel samples with different textures: open circles correspond to the {100}⟨001⟩ + {121}⟨011⟩ texture and full circles represent the {132}⟨112⟩ texture. The starting material was 80 %RA nickel and the magnetic treatment was low-field/high-frequency at room temperature.

the associated increase in the size of the error bars for the *R*-values in the grain-growth region. Despite the breakdown of both *S*- and *R*-analysis in the grain-growth region, it is interesting to note the sudden increase in the *R*-parameter at 400 °C.

These experiments confirm the ability of DBPAS to monitor effectively both the changes in point-defect concentration during recovery and changes in dislocation concentration during the recrystallization stage of the thermal annealing process.

The data in figure 4 suggest that the magnetic treatment has no significant effect on the point-defect concentration of the quenched samples since the *S*- and *R*-parameters remain constant within the experimental error. The prior results from the PAS experiments on the thermally annealed samples (recovery stage) allows one to rule out the possibility that PAS is simply unable to track the relevant changes in point-defect concentrations.

Figures 5–7 show a decrease in the *S*-parameter while the *R*-parameter remains constant for various combinations of magnetic processing parameters. These decreases, together with the previous observation that magnetic treatment does not significantly affect point defects, suggests that the magnetic processing is causing a decrease in the dislocation density. We believe that the interaction between the stress field of a moving domain wall and that of a dislocation can be of sufficient magnitude to cause dislocation motion. Seeger *et al* [14, 17] and Trauble [16] have shown that the magnitude of the shear stress exerted by the domain wall on the dislocation is ~ 1.3 kg mm^{-2}. Since this value is larger than the critical resolved shear stress of nickel (~ 0.80 kg mm^{-2} at 77 K and ~ 0.70 kg mm^{-2} at 300 K [18]), it is reasonable to believe that the cyclic magnetization process may result in dislocation motion.

Previous work by Craik and Tebble [19] and Lilley [20] suggests that the domain-wall structure and, therefore, the magnitude of the force of interaction between the domain walls and the dislocations, is a function of the texture of the sample. Thus, it appears that an

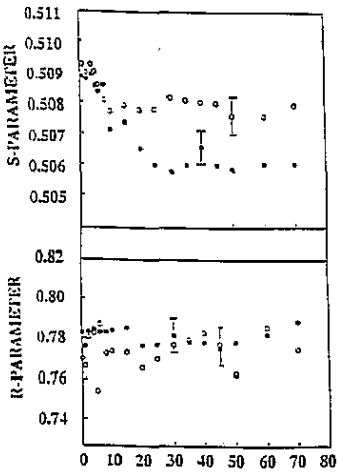

Figure 6. *S*- and *R*-parameters as a function of number of rounds of magnetic treatment for nickel samples magnetically processed at different temperatures: open circles correspond to room temperature and full circles to treatment at 77 K. The starting material was 80 %RA nickel with the {132}⟨112⟩ texture and the low-field/high-frequency magnetic treatment was employed.

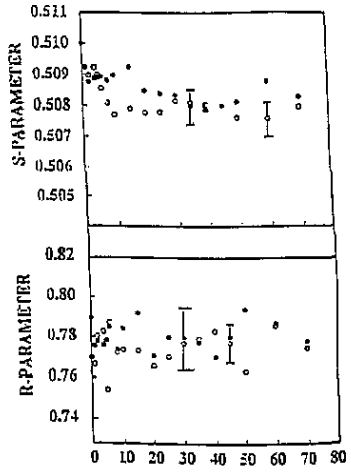

Figure 7. *S*- and *R*-parameters as a function of number of rounds of magnetic treatment for nickel samples magnetically processed at different field strengths and frequencies: open circles correspond to low-field/high-frequency and full circles to high-field/low-frequency. The starting material was 80 %RA nickel with the {132}⟨112⟩ texture and the magnetic processing was performed at room temperature.

influence of texture on the extent of magnetically induced recovery is expected. Figure 5 shows that the decrease in dislocation density is more predominant in the samples with {132}⟨112⟩ texture than in the similar samples with the {100}⟨001⟩ + {121}⟨011⟩ texture. Our modelling work has not progressed to the point where we can quantitatively explain this result.

Figure 6 shows that the extent of recovery is more pronounced at 77 K. This may be because of the decrease in thermal agitation resulting in a stronger cooperative interaction between magnetic moments. This would result in a more extensive change in the domain pattern and consequently a larger interaction between dislocations and domain walls. We believe that there may be an optimum temperature for the magnetic recovery process due to the competing influence of temperature on ease of dislocation motion and strength of magnetic interactions.

Due to instrument limitations associated with the fluxatron the effects of field strength and frequency were not investigated independently. As shown in figure 7, the amount of magnetic recovery (as measured by a reduction in the *S*-parameter) is slightly more pronounced in the low-field and high-frequency combination than in the high-field and low-frequency treatment. We note, however, that the magnitude of the difference between the *S*-parameters for the two treatments is similar to the size of the error bars, so that additional experimental evidence is necessary before any definite conclusions can be reached. Field strength could be important since higher fields can result in domain growth and, therefore, in a decrease in the extent of domain-wall–dislocation interaction. The optimum processing frequency may be related to the maximum dislocation velocity in the material. It is also possible that different field strength–frequency combinations may result in different amounts of sample heating during magnetic processing. Although we did not measure temperature

changes during magnetic processing, no significant increases were apparent. Additional experiments are planned to permit the separation of the influences of field strength and frequency on the magnetic recovery process.

6. Conclusions

This work has attempted to identify the type of defect associated with recovery and also to identify the important processing parameters that affect the extent of magnetic recovery. The results indicate that the magnetic processing causes a more substantial change in the dislocation structure of the material than in the point-defect density. This conclusion is based on the following experimental observations:

(i) PAS is capable of following the reduction in point-defect concentration that occurs when quenched samples are thermally annealed;

(ii) PAS is capable of following the reduction in both the point-defect concentration and dislocation concentration that occurs when a heavily cold worked sample is thermally annealed;

(iii) PAS shows no significant changes in defect structure when quenched samples are magnetically annealed (i.e. magnetic annealing does not significantly influence point-defect structures); and

(iv) PAS reveals changes in defect structures when cold worked samples are magnetically annealed (i.e. if PAS is not responding to changes in point-defect structures it is likely that it is responding to changes in dislocation structures).

Of the experimental variables investigated, temperature and texture seem to have the most significant influence on the extent of magnetically induced recovery. Additional work is required to model the magnetic recovery process accurately. The authors at Lafayette are currently engaged in identifying the optimum temperature, field strength and frequency through additional experimentation and preliminary models. An energy approach to relate the magnetic energy from the pulsed field to the activation energy obtained from differential calorimetry experiments is also under way.

References

[1] Hayashi S, Takahashi S and Yamamoto M 1971 *J. Phys. Soc. Japan* **30** 2

[2] Philip A H 1984 *Mater. Sci. Eng.* **64** L23–6

[3] Kovaleva T G, Polandova A N, Smorodin V I, Kovalev A I and Shevchuk A D 1985 *Strength Mater.* **17** 50–2

[4] Jablonowski J 1987 *Am. Mach. Autom. Manuf.* 80–2

[5] Hochman R F, Tselesin N and Drits V 1988 *Adv. Mater. Process.* **134** 36–41

[6] Su Y Y, Hochman R F and Schaffer J P 1990 *J. Phys.: Condens. Matter* **2** 3629–42

[7] West R N 1974 *Positron Studies of Condensed Matter* (London: Taylor and Francis)

[8] Eldrup M 1985 *Defects in Solids* ed A V Chadwick and M Terenzi (New York: Plenum)

[9] Mackenzie I M 1983 *Experimental Methods of Annihilation Time and Energy Spectrometry in Positron Solid-State Physics* ed W Brandt and A Dupasquire (Amsterdam: North-Holland)

[10] Chen C W 1986 *Magnetism and Metallurgy of Soft Magnetic Materials* (New York: Dover)

[11] Cullity B D 1972 *Introduction to Magnetic Materials* (Reading, MA: Addison-Wesley)

[12] MacKenzie I K, Eady J A and Gingerich R R 1970 *Phys. Lett.* **33A** 279

[13] Mantl S and Triftshauser W 1978 *Phys. Rev.* B **17** 1645–52

[14] Seeger A and Kronmuller H 1987 *Mater. Sci. Forum* **15–18** 65–70

[15] Clarebrough L M, Hargreaues M E and Loretto M H 1963 *Conference on Recovery and Recrystallization of Metals* ed L Himmel (New York: Interscience)
[16] Trauble H 1967 *Magnetism and Metallurgy* ed A E Berkowitz and E Kneller (London: Academic)
[17] Seeger A, Kronmuller H, Rieger H and Trauble H 1964 *J. Appl. Phys.* **35** 740
[18] Haasen P 1958 *Phil. Mag.* **3** 384
[19] Craik D J and Tebble R S 1965 *Ferromagnetism and Ferromagnetic Domains* (Amsterdam: North-Holland) pp 109, 204
[20] Lilley B A 1950 *Phil. Mag.* **41** 792